

Simultaneous field-free molecular orientation and planar delocalization by THz laser pulses [Invited]

Dominique Sugny*

Laboratoire Interdisciplinaire Carnot de Bourgogne (ICB), UMR 6303 CNRS-Université Bourgogne Franche Comté, F-21078 Dijon, France

*Corresponding author: dominique.sugny@u-bourgogne.fr

Received August 12, 2022 | Accepted September 2, 2022 | Posted Online October 20, 2022

This study shows the unexpected and counterintuitive possibility of simultaneously orienting a molecule while delocalizing its molecular axis in a plane in field-free conditions. The corresponding quantum states are characterized, and different control strategies using shaped terahertz (THz) laser pulses are proposed to reach such states at zero and nonzero temperatures. The robustness against temperature effects of a simple control procedure combining a laser and a THz pulse is shown. Such control strategies can be applied not only to linear molecules but also to symmetric top molecules.

Keywords: rotational dynamics; quantum control; molecular orientation and alignment; THz laser pulses.

DOI: [10.3788/COL202220.100008](https://doi.org/10.3788/COL202220.100008)

1. Introduction

Quantum control tackles the question of bringing a quantum system from one state to another by means of external electromagnetic pulses. It has now become a well-recognized area of research, with applications ranging from chemistry and quantum technologies to materials science and nanotechnology^[1–3]. In molecular physics, quantum control has been used in a large number of studies for manipulating molecular rotation, in particular to enhance molecular alignment and orientation in gas phase (see Refs. [4–8] and references therein). The control of such phenomena is key because they play a crucial role in a wide variety of domains such as chemical reaction dynamics, surface processing, catalysis and quantum computing, to cite a few. In the case of a linear molecule driven by a linearly polarized laser field, alignment means an increased probability distribution along the polarization axis, whereas orientation requires, in addition, the same or opposite direction as the polarization vector. Field-free alignment and orientation are investigated in this paper^[7]. It is worth noting that for experiments requiring conditions without external electromagnetic fields, noticeable orientation and alignment that persist after the end of the pulse are of special importance. In this description, it seems obvious that any oriented state is also aligned, while the converse is not true. Indeed, an aligned state can be defined as a quantum superposition of two oriented states along opposite directions. This study shows that this first statement is not entirely valid, since there exist oriented states that can be (to some extent) also characterized by planar delocalization.

From a more general perspective, the control of molecular alignment is nowadays well understood in the adiabatic or

sudden regime^[4,5,9–12] by means of laser pulses. In the past few years, different studies have extended the standard control framework by considering, e.g., the deflection of aligned molecules^[13], collisional effects on quantum dynamics^[14–16], or rotational echoes^[17]. The shaping of field-free alignment dynamics has also been extensively investigated. A series of nontrivial extensions have been proposed. They go from planar alignment^[18], unidirectional rotation of the molecular axis^[19–21], and alignment alternation^[22] to the control of rotational wave packet dynamics^[23]. The control of molecular orientation is not at the same stage of maturity even if, on the theoretical side, several control protocols to enhance the degree of orientation have been developed and applied with success^[24–49]. Some of them have been implemented experimentally^[50–57], in particular in field-free conditions by using terahertz (THz) laser fields^[50,51]. It is worth noting that most of the control strategies developed so far have only investigated the optimization of the degree of orientation without generating other dynamics^[58].

This paper explores another aspect of field-free molecular orientation, that is, the unexpected and counterintuitive possibility of orienting a molecule while delocalizing its molecular axis in a plane orthogonal to the orientation direction. Introducing a new observable combining the degrees of orientation and alignment of the system, the corresponding quantum states are identified as specific eigenvectors of this operator. They are then completely characterized, both from a classical and a quantum point of view. The physical limits to this simultaneous dynamic are also established. Using optimal control theory (OCT)^[1,2], a THz field that brings the system to the target state is designed at zero temperature. Such optimal solutions are of remarkable efficiency, close to 100%. Numerical results are presented for the CO molecule.

Despite its relative complexity, the control procedure could be, in principle, experimentally implemented by standard pulse-shaping techniques. A less demanding quantum state that is oriented but not aligned is considered at nonzero temperature. A simple bipulse process is then proposed to generate these states. It is composed of a short laser pulse followed by a THz half-cycle pulse (HCP)^[7] after a quarter rotational period. It is shown that this control strategy is efficient, robust to temperature effects, and experimentally easier to implement. This control procedure is applied to the linear CO molecule but also to a symmetric top molecule, CH₃I.

The paper is organized as follows. The quantum states leading simultaneously to orientation and planar delocalization are characterized and described in Section 2. Different control strategies to reach these states are proposed in Section 3, both at zero and nonzero temperatures. Conclusions and prospective views are given in Section 4.

2. Description of the Classical and Quantum States

The time evolution of the rotation of a polar linear molecule subjected to a linearly polarized THz pulse of amplitude $E(t)$ at zero temperature is governed by the following Schrödinger equation written in the rigid rotor approximation^[7]:

$$i \frac{d}{dt} |\psi(t)\rangle = H |\psi(t)\rangle,$$

with $|\psi(t)\rangle$ the state of the system and the Hamiltonian H given by

$$H = B J^2 - \mu_0 \cos \theta E(t),$$

where B and μ_0 are, respectively, the rotational constant and the permanent dipole moment. J^2 is the angular momentum operator and θ the polar angle between the molecular axis and the field polarization direction corresponding to the z axis of the laboratory frame (x, y, z) . The eigenvectors of J^2 in this frame are denoted $|jm\rangle$ with $j \geq 0$ and $-j \leq m \leq j$, the z axis being the quantum axis used to define these rotational states. Note that the units used throughout this paper are atomic units unless otherwise specified. The degrees of orientation and alignment are, respectively, measured by $\langle \cos \theta \rangle$ and $\langle \cos^2 \theta \rangle$. In field-free conditions, the two expectation values oscillate with a period π/B corresponding to the rotational period of the molecule. A planar delocalization is achieved when $\langle \cos^2 \theta \rangle < \frac{1}{3}$ (1/3 being the degree of alignment at thermal equilibrium), while the molecule is said to be oriented along the z axis if $\langle \cos \theta \rangle \simeq \pm 1$, or at least if $\langle \cos \theta \rangle \neq 0$.

Field-free simultaneous orientation and planar delocalization combine at the same time as the degrees of orientation and alignment. The corresponding observable therefore both depends on $\cos \theta$ and $\cos^2 \theta$. This choice is not unique, but a convenient one is the observable F defined as

$$F = \cos \theta - a \cos^2 \theta,$$

where a is a positive parameter that expresses the relative weight between the orientation and the alignment of the state. At this point, it is clear that the targeted quantum state must maximize $\langle F \rangle$. A first analysis of the behavior of F can be done in the classical limit. In this case, the maximum of F occurs for $\theta_{\max} = a \cos(\frac{1}{2a})$, leading to $\cos \theta_{\max} = \frac{1}{2a}$. Figure 1 displays the evolution of the two classical observables with respect to a . It can be deduced that the value of a , which maximizes F , is $a = \frac{1}{2}$ for $\theta_{\max} = 0$ and $\cos \theta_{\max} = \cos^2 \theta_{\max} = 1$. In this case, simultaneous molecular orientation and alignment are achieved. Isotropic distribution of the probability density is obtained for $\cos^2 \theta = \frac{1}{3}$, which gives $a = \frac{\sqrt{3}}{2}$ and $\cos \theta = \frac{1}{\sqrt{3}}$, as indicated in Fig. 1. More interestingly, when $a > \frac{\sqrt{3}}{2}$, a planar delocalization for an oriented state is produced with $\cos^2 \theta < \frac{1}{3}$ and $\cos \theta > 0$. The results can be summarized as follows.

- For $a \in [\frac{1}{2}, \frac{\sqrt{3}}{2}]$, the molecule is aligned and oriented with $\cos^2 \theta \geq 1/3$ and $\cos \theta > 0$.
- For $a \geq \frac{\sqrt{3}}{2}$, the molecule is delocalized and oriented with $\cos^2 \theta \leq 1/3$ and $\cos \theta > 0$.

It is shown below that such classical limits give a good estimate of the expectation values of the observables that can be achieved in the quantum regime.

The next step is to describe this phenomenon in the quantum setting. A major mathematical difficulty of this description comes from the infinite-dimensional Hilbert space of the rotational system. This problem is circumvented by considering a reduction of the original Hilbert space to a finite-dimensional one. From a physical point of view, this reduction can be justified

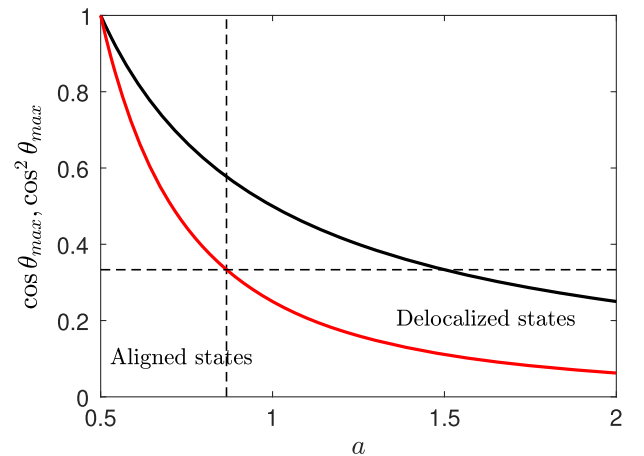


Fig. 1. Evolution of $\cos \theta_{\max}$ (black line) and $\cos^2 \theta_{\max}$ (red line) as a function of the parameter a . θ_{\max} is the angle that maximizes the figure of merit F for a given value of a . The horizontal dashed line delimits the region of aligned and delocalized states. The area to the right of the vertical dashed line (of equation $a = \frac{\sqrt{3}}{2}$) corresponds to simultaneous orientation and planar delocalization.

by the fact that the system is only subjected to a finite number of applied pulses with moderate amplitude. Since such pulses transfer finite amounts of energy to the system, this latter stays thus essentially confined in a finite-dimensional subspace. This reduction considerably simplifies the definition of the target state and the analysis of its properties. Note that the strategy used in this paper emerges as a specific example of a more general analysis already applied to maximize, e.g., molecular orientation and alignment^[59–62]. A natural reduction of the Hilbert space consists in introducing a finite Hilbert space $\mathcal{H}_{j_{\max}}$, spanned by the lowest rotational states $\{|j, m\rangle, j \leq j_{\max}\}$. The idea is then to identify the target state $|\psi_T\rangle$ in $\mathcal{H}_{j_{\max}}$, with $m = 0$, as the state maximizing the simultaneous orientation and planar delocalization in this subspace, i.e., maximizing $\langle \psi_T | P_{j_{\max}} F P_{j_{\max}} | \psi_T \rangle$, where $P_{j_{\max}}$ is the projector onto the space $\mathcal{H}_{j_{\max}}$. It is then straightforward to show that this state corresponds to the eigenvector of $P_{j_{\max}} F P_{j_{\max}}$ with the highest eigenvalue^[59]. Note that this method can be generalized to density matrices at nonzero temperatures^[60]. However, this generalization is not straightforward because, in this case, the state of the system is described by a density matrix (see Section 3 for technical details). The idea would then be to find the density operator that maximizes the expectation value of the observable F , while being linked to the initial state by unitary evolution. This leads to a rather involved computation, which is beyond the scope of this paper.

This general discussion is illustrated by a series of numerical results on a fictive molecule with $B = 1$. Figure 2 displays the maximum of $\langle \cos \theta \rangle$ and $\langle \cos^2 \theta \rangle$ with respect to the two parameters j_{\max} and a . Two different zones can be clearly distinguished. A region of simultaneous high degrees of orientation and alignment can be found in the top left part of the two panels. This zone corresponds typically to small values of a , lower than 1. More unexpected, a flat zone for $a \geq 2$ and $j_{\max} \geq 7$ also appears in the right parts of Fig. 2. In this case, $\langle \cos^2 \theta \rangle < \frac{1}{3}$ so the molecule is delocalized in the (x, y) plane, but with a noticeable orientation larger than 0.2.

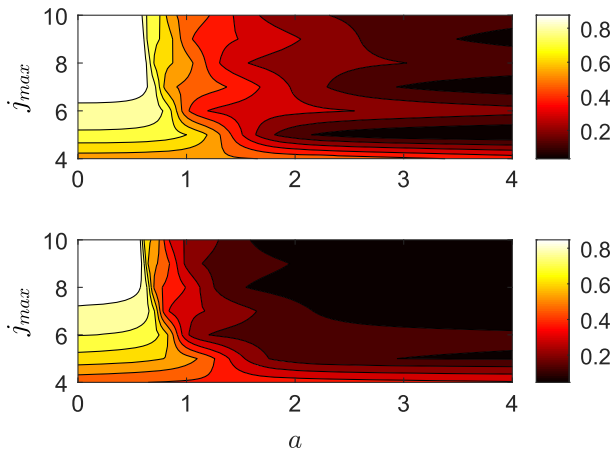


Fig. 2. Contour plot of the maximum of $\langle \cos \theta \rangle$ (top panel) and $\langle \cos^2 \theta \rangle$ (bottom panel) as a function of a and j_{\max} .

More insight about this unusual behavior is given in Fig. 3, with the probability density of $|\psi_T\rangle$. This density has the shape of a bowl without handle and with a rotational symmetry around the z axis. It clearly corresponds to an oriented state, since the probability density belongs to the subspace with $z \geq 0$. However, the flared shape of the bowl allows at the same time to have a noticeable planar delocalization in the (x, y) plane. This density is also very different from those obtained with oriented and aligned states that have a cigar shape along the z axis.

Note that there exists a target state for every value of j_{\max} , but with very similar properties when $j_{\max} \geq 7$. The state that is generally reached by a control process features a quantum superposition of different target states.

Another interesting characteristic of $|\psi_T\rangle$ can be found in Fig. 4, in which the degrees of orientation and alignment are

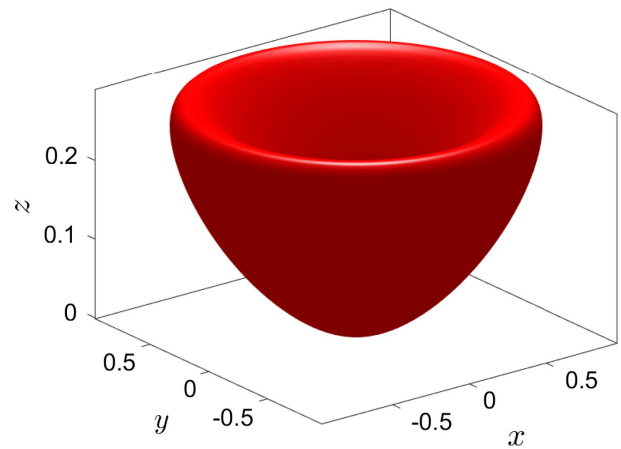


Fig. 3. Probability density of the quantum state $|\psi_T\rangle$ maximizing the orientation and the planar delocalization simultaneously for $a = 2$ and $j_{\max} = 10$.

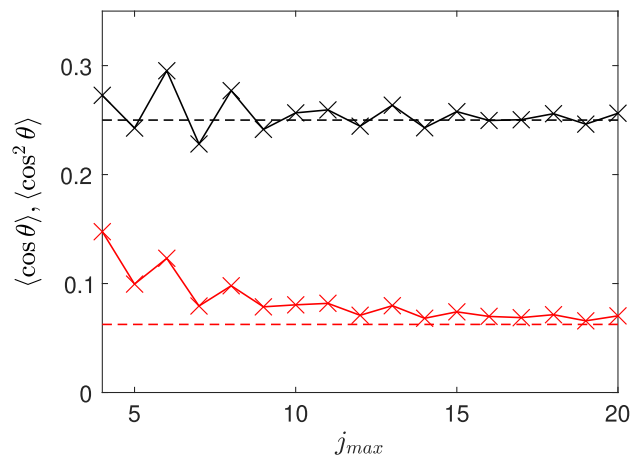


Fig. 4. Evolution of the expectation values $\langle \cos \theta \rangle$ (black line) and $\langle \cos^2 \theta \rangle$ (red line) in the state $|\psi_T\rangle$ of a fictive molecule as a function of j_{\max} for $a = 2$ (crosses). The solid lines are just to guide the reader. The horizontal dashed lines represent the classical values of $\cos \theta$ and $\cos^2 \theta$ for $\theta_{\max} = \frac{1}{2a}$.

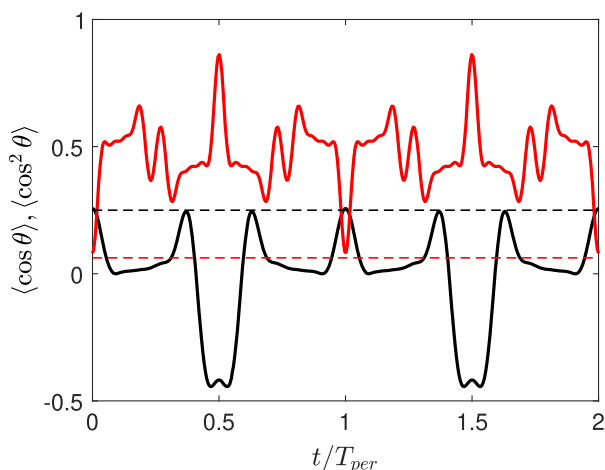


Fig. 5. Field-free time evolution of the expectation values $\langle \cos \theta \rangle$ (black line) and $\langle \cos^2 \theta \rangle$ (red line) of a fictive molecule at $T = 0$ K. The initial state at $t = 0$ is $|\psi_T\rangle$. The parameters a and j_{max} are set to 2 and 10. The horizontal dashed lines represent the classical values of $\cos \theta$ and $\cos^2 \theta$ for $\theta_{\text{max}} = \frac{1}{2a}$.

plotted as a function of j_{max} for a fixed value of a . It can be seen that for $j_{\text{max}} \geq 10$, the two quantum expectation values are almost constant and very close to their classical estimates given in Fig. 1. This result confirms the fact that this state depends little on the value of j_{max} and that useful information can be gained from a classical analysis of the rotational dynamics. As already mentioned, the choice of the parameter a allows one to weight the relative importance of orientation and planar delocalization in the target state.

Figure 5 gives a view of the rotational dynamics starting from $|\psi_T\rangle$. Different revivals of simultaneous orientation and delocalization are observed at multiple times of T_{per} . Note that it is only around such times that $\langle \cos^2 \theta \rangle < \frac{1}{3}$. Here again, the quantum expectation values are very close to their classical counterparts. At revival times $t = (2n + 1) \frac{T_{\text{per}}}{2}$ for integers n , the dynamics goes through a state that is aligned and oriented.

3. Control of Simultaneous Orientation and Planar Delocalization at Zero and Nonzero Temperatures

Having defined the target states, the next step consists in designing control strategies to reach a given target state or a superposition of such states. Control fields using OCT^[1,3,63] are first computed. A standard gradient-based iterative algorithm whose efficiency has been shown in a variety of studies for rotational dynamics^[3,12,25] is applied to the CO molecule. Molecular parameters are taken to be $B = 1.9313 \text{ cm}^{-1}$ and $\mu_0 = 0.112 \text{ D}$. As an illustrative example, a pulse duration of one rotational period and a target state corresponding to $j_{\text{max}} = 10$ and $a = 2$ are considered. Similar results have been obtained for other values of j_{max} and a . The goal of the control process is to maximize the projection of the final state onto the target. A Gaussian pulse

centered at $t_0 = T_{\text{per}}/5$ is taken as a guess field for the optimization procedure with $E(t) = E_0 e^{-\frac{(t-t_0)^2}{2\sigma^2}}$, where $I_0 = 20 \text{ TW/cm}^2$ is the maximum intensity of the electric field and $\sigma = \pi/(50B)$. A final projection larger than 0.99 has been achieved. Figure 6 displays the results of the optimization procedure, with the optimal solution computed by the algorithm. A simultaneous orientation and planar delocalization is obtained at $t = T_{\text{per}}$ when the control field is switched off.

In view of experimental applications, it is also interesting to find simpler strategies composed of a series of short pulses. Even if these control processes have an efficiency that is less than that of optimal control, they also have the decisive advantage of being robust with respect to experimental constraints, such as temperature effects. A control procedure at nonzero temperatures is now investigated. In this case, the quantum system is described by a density operator $\rho(t)$ whose dynamics is governed by the von Neumann equation^[7],

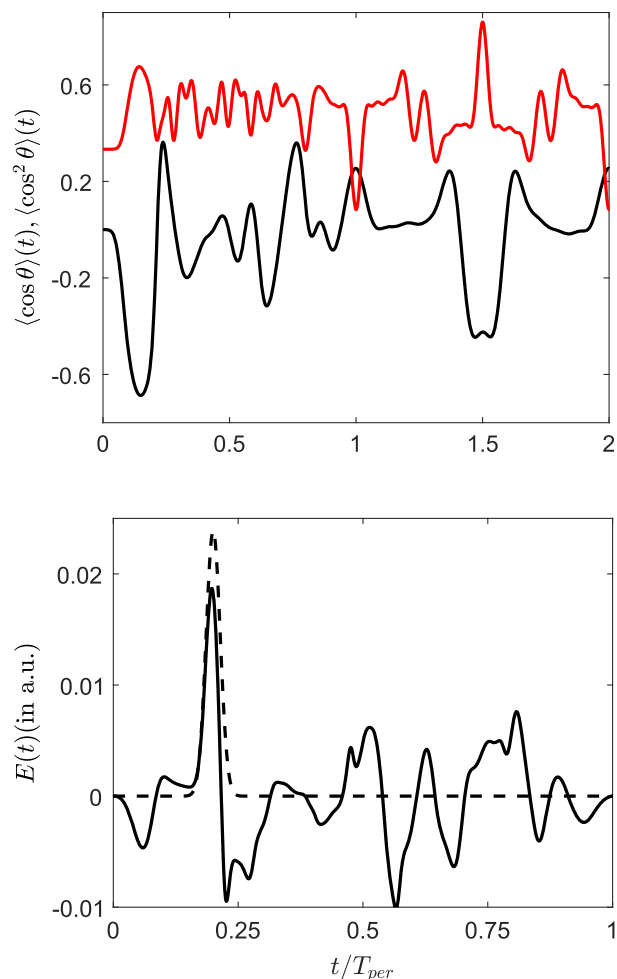


Fig. 6. (Top) Time evolution of $\langle \cos \theta \rangle$ (black line) and $\langle \cos^2 \theta \rangle$ (red line) for the CO molecule at $T = 0$ K under the action of the optimized pulse (bottom) followed by a field-free evolution of one rotational period. Numerical parameters are set to $a = 2$ and $j_{\text{max}} = 10$.

$$i \frac{d\rho}{dt} = [H(t), \rho].$$

The initial condition at $t = 0$, i.e., when the laser is switched on, is the Boltzmann distribution,

$$\rho(0) = \frac{1}{Z} \sum_{j=0}^{\infty} \sum_{m=-j}^j e^{-Bj(j+1)/(k_B T)} |jm\rangle \langle jm|,$$

where $Z = \sum_{j=0}^{\infty} \sum_{m=-j}^j e^{-Bj(j+1)/(k_B T)}$ is the partition function, k_B the Boltzmann constant, and T the temperature of the sample. Here, the degree of orientation is given by $\langle \cos \theta \rangle = \text{Tr}[\rho \cos \theta]$. At nonzero temperatures, it is difficult to reach states that are both oriented and with a planar delocalization. Note that the target states defined at zero temperature in Section 2 could be generalized to the density matrix formalism using the results described in Ref. [60]. However, the computation is rather involved and leads to complex pulses. To limit the

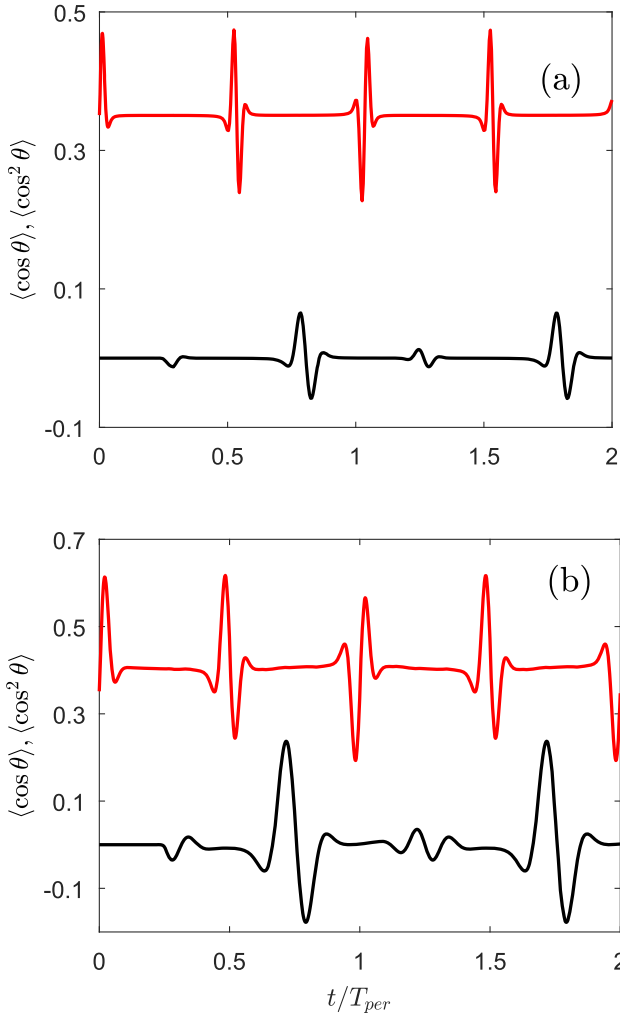


Fig. 7. Time evolution of $\langle \cos \theta \rangle$ (black line) and $\langle \cos^2 \theta \rangle$ (red line) for the CO molecule at $T = 200$ K [panel (a)] and 30 K [panel (b)] generated by a laser pulse followed by an HCP.

complexity of the control processes, the idea is thus to relax these conditions and to consider less demanding states that are oriented but not aligned, i.e., with $\langle \cos^2 \theta \rangle \simeq 1/3$. A simple control strategy can be used toward this aim. It is based on the application of a short laser pulse followed by an HCP; the two pulses are temporally delayed by $T_{per}/4$. The two pulses are Gaussian and linearly polarized along the z axis. Note that similar control procedures have been proposed to enhance molecular orientation^[26,64,65]. Numerical results are displayed in Fig. 7 for the CO molecule at two different temperatures. The intensity of the laser is 50 TW/cm^2 with a duration (FWHM) of 50 fs, while the HCP has a duration of 100 fs, the corresponding electric field having a peak amplitude of 10^8 V/m . It can be seen in Fig. 7 that the first laser field at time $t = 0$ produces a nonadiabatic alignment, featured by revivals occurring at fractional times of the rotational period (multiples of $T_{per}/2$). The second pulse breaks the symmetry of the dynamics and generates oriented states. The collective action of the two pulses results in a transient orientation at times $T_{per}/4 + nT_{per}$, for integers n , with an alignment equal to the permanent alignment of the molecule. The dynamic alternates between an aligned state with no orientation and an oriented state with only a permanent alignment. Note that the control process is robust with respect to temperature, as shown in Fig. 7, in which the same control procedure has been used at two different temperatures. This phenomenon can be enhanced to some extent by using a laser pulse followed by a train of HCPs applied at times $T_{per}/4 + nT_{per}/2$ with adjusted intensity^[10,59].

The control strategy extends to symmetric top molecules, as illustrated in Fig. 8, for the CH_3I molecule at $T = 30$ K. In the control process, the intensity of the laser is set to 50 TW/cm^2 , and the HCP is replaced by a single-cycle THz pulse of peak amplitude $2 \times 10^7 \text{ V/m}$. This latter pulse has been recently used experimentally to orient this molecule (see Ref. [51] for the molecular parameters and technical details). Here again, a

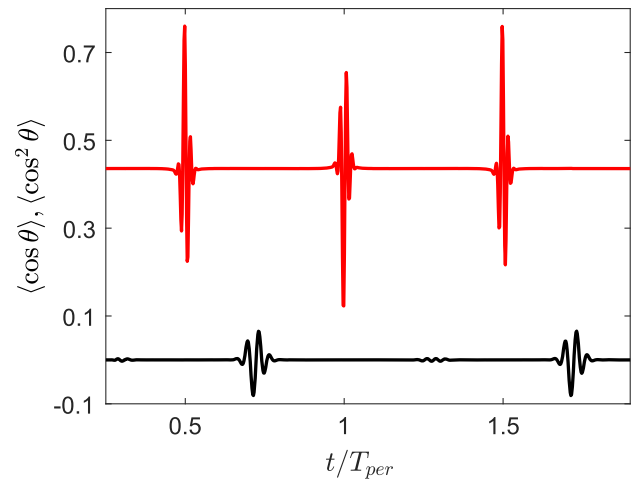


Fig. 8. Same as Fig. 7, but for the CH_3I molecule at $T = 30$ K. The HCP is replaced by a single-cycle pulse in the control process. Note that the range of time starts at time $t/T_{per} = 0.25$ in order to highlight the field-free evolution.

noticeable orientation is achieved with only a permanent alignment. The robustness against temperature effects and variations of pulse amplitude has been also verified.

4. Conclusion

This study has investigated the extent to which a molecule can be simultaneously oriented and delocalized in a plane in field-free conditions. After a classical description of the phenomenon, the corresponding quantum states have been described in detail at zero temperature. Such target states can be reached with a very good efficiency by using optimal control procedures, the price to pay being a relatively complex control pulse. The efficiency of this method is only limited by the maximum field intensity, which can be used to prevent molecular ionization. At nonzero temperatures, a simpler control strategy has been proposed allowing the generation of less demanding dynamics. This procedure can be used for linear molecules and also symmetric top molecules. Such a phenomenon is interesting from a fundamental point of view, and it allows one to show that unexpected results can be obtained in the quantum regime by shaping the probability density of the rotational states at will^[58]. Finally, it should be possible to reach such states by using a spectrally shaped two-color laser pulse^[30,54]. This issue, which goes beyond the scope of this study, is an interesting generalization of the results presented in this paper.

Acknowledgement

I thank Dr. M. Lapert and M. Ndong for many helpful discussions and for providing me with the idea at the origin of this paper.

References

1. S. J. Glaser, U. Boscain, T. Calarco, C. P. Koch, W. Köckenberger, R. Kosloff, I. Kuprov, B. Luy, S. Schirmer, T. Schulte-Herbrüggen, D. Sugny, and F. K. Wilhelm, "Training Schrödinger's cat: quantum optimal control," *Eur. Phys. J. D* **69**, 279 (2015).
2. C. P. Koch, U. Boscain, T. Calarco, G. Dirr, S. Filipp, S. J. Glaser, R. Kosloff, S. Montangero, T. Schulte-Herbrüggen, D. Sugny, and F. K. Wilhelm, "Quantum optimal control in quantum technologies. Strategic report on current status, visions and goals for research in Europe," *EPJ Quantum Technol.* **9**, 19 (2022).
3. C. Brif, R. Chakrabarti, and H. Rabitz, "Control of quantum phenomena: past, present and future," *New J. Phys.* **12**, 075008 (2010).
4. H. Stapelfeldt and T. Seideman, "Colloquium: aligning molecules with strong laser pulses," *Rev. Mod. Phys.* **75**, 543 (2003).
5. T. Seideman and E. Hamilton, "Nonadiabatic alignment by intense pulses. concepts, theory, and directions," *Adv. At. Mol. Opt. Phys.* **52**, 289 (2005).
6. M. Lemeshko, R. Krems, J. Doyle, and S. Kais, "Nonadiabatic alignment by intense pulses. concepts, theory, and directions," *Mol. Phys.* **111**, 1648 (2013).
7. C. P. Koch, M. Lemeshko, and D. Sugny, "Quantum control of molecular rotation," *Rev. Mod. Phys.* **91**, 035005 (2019).
8. V. V. Nautiyal, S. Devi, A. Tyagi, B. Vidhani, A. Maan, and V. Prasad, "Orientation and alignment dynamics of polar molecule driven by shaped laser pulses," *Spectrochim. Acta A* **256**, 119663 (2021).
9. B. Friedrich and D. Herschbach, "Alignment and trapping of molecules in intense laser fields," *Phys. Rev. Lett.* **74**, 4623 (1995).
10. M. Leibscher, I. S. Averbukh, and H. Rabitz, "Molecular alignment by trains of short laser pulses," *Phys. Rev. Lett.* **90**, 213001 (2003).
11. M. Leibscher, I. S. Averbukh, and H. Rabitz, "Enhanced molecular alignment by short laser pulses," *Phys. Rev. A* **69**, 013402 (2004).
12. J. Salomon, C. M. Dion, and G. Turinici, "Optimal molecular alignment and orientation through rotational ladder climbing," *J. Chem. Phys.* **123**, 144310 (2005).
13. E. Gershnel and I. S. Averbukh, "Deflection of field-free aligned molecules," *Phys. Rev. Lett.* **104**, 153001 (2010).
14. S. Ramakrishna and T. Seideman, "Intense laser alignment in dissipative media as a route to solvent dynamics," *Phys. Rev. Lett.* **95**, 113001 (2005).
15. T. Viellard, F. Chaussard, D. Sugny, B. Lavorel, and O. Faucher, "Field-free molecular alignment of CO₂ mixtures in presence of collisional relaxation," *J. Raman Spectrosc.* **39**, 694 (2008).
16. T. Viellard, F. Chaussard, F. Billard, D. Sugny, O. Faucher, S. Ivanov, J.-M. Hartmann, C. Boulet, and B. Lavorel, "Field-free molecular alignment for probing collisional relaxation dynamics," *Phys. Rev. A* **87**, 023409 (2013).
17. G. Karras, E. Hertz, F. Billard, B. Lavorel, J.-M. Hartmann, O. Faucher, E. Gershnel, Y. Prior, and I. S. Averbukh, "Orientation and alignment echoes," *Phys. Rev. Lett.* **114**, 153601 (2015).
18. M. Z. Hoque, M. Lapert, E. Hertz, F. Billard, D. Sugny, B. Lavorel, and O. Faucher, "Observation of laser-induced field-free permanent planar alignment of molecules," *Phys. Rev. A* **84**, 013409 (2011).
19. O. Korech, U. Steinitz, R. J. Gordon, I. S. Averbukh, and Y. Prior, "Observing molecular spinning via the rotational Doppler effect," *Nat. Photonics* **7**, 711 (2013).
20. U. Steinitz, Y. Prior, and I. S. Averbukh, "Optics of a gas of coherently spinning molecules," *Phys. Rev. Lett.* **112**, 013004 (2014).
21. G. Karras, M. Ndong, E. Hertz, D. Sugny, F. Billard, B. Lavorel, and O. Faucher, "Polarization shaping for unidirectional rotational motion of molecules," *Phys. Rev. Lett.* **114**, 113001 (2015).
22. D. Daems, S. Guérin, E. Hertz, H. R. Jauslin, B. Lavorel, and O. Faucher, "Field-free two-direction alignment alternation of linear molecules by elliptic laser pulses," *Phys. Rev. Lett.* **95**, 063005 (2005).
23. M. Spanner, E. A. Shapiro, and M. Ivanov, "Coherent control of rotational wave-packet dynamics via fractional revivals," *Phys. Rev. Lett.* **92**, 093001 (2004).
24. I. S. Averbukh and R. Arvieu, "Angular focusing, squeezing, and rainbow formation in a strongly driven quantum rotor," *Phys. Rev. Lett.* **87**, 163601 (2001).
25. L. H. Coudert, "Optimal orientation of an asymmetric top molecule with terahertz pulses," *J. Chem. Phys.* **146**, 024303 (2017).
26. D. Daems, S. Guérin, D. Sugny, and H. R. Jauslin, "Efficient and long-lived field-free orientation of molecules by a single hybrid short pulse," *Phys. Rev. Lett.* **94**, 153003 (2005).
27. C. M. Dion, A. Keller, and O. Atabek, "Optimally controlled field-free orientation of the kicked molecule," *Phys. Rev. A* **72**, 023402 (2005).
28. M. Lapert and D. Sugny, "Field-free molecular orientation by terahertz laser pulses at high temperature," *Phys. Rev. A* **85**, 063418 (2012).
29. D. Sugny, S. Vranckx, M. Ndong, N. Vaecq, O. Atabek, and M. Desouter-Lecomte, "Control of molecular dynamics with zero-area fields: application to molecular orientation and photofragmentation," *Phys. Rev. A* **90**, 053404 (2014).
30. R. Tehini and D. Sugny, "Field-free molecular orientation by nonresonant and quaresonant two-color laser pulses," *Phys. Rev. A* **77**, 023407 (2008).
31. R. Tehini, M. Z. Hoque, O. Faucher, and D. Sugny, "Field-free molecular orientation of and molecules at high temperature," *Phys. Rev. A* **85**, 043423 (2012).
32. N. E. Henriksen, "Molecular alignment and orientation in short pulse laser fields," *Chem. Phys. Lett.* **312**, 196 (1999).
33. Q.-Q. Hong, L.-B. Fan, C.-C. Shu, and N. E. Henriksen, "Generation of maximal three-state field-free molecular orientation with terahertz pulses," *Phys. Rev. A* **104**, 013108 (2021).
34. K. Kitano, N. Ishii, and J. Itatani, "High degree of molecular orientation by a combination of THz and femtosecond laser pulses," *Phys. Rev. A* **84**, 053408 (2011).

35. H. Li, W. Li, Y. Feng, H. Pan, and H. Zeng, "Field-free molecular orientation by femtosecond dual-color and single-cycle THz fields," *Phys. Rev. A* **88**, 013424 (2013).
36. J. J. Omiste and R. Gonzalez-Ferez, "Theoretical description of the mixed-field orientation of asymmetric-top molecules: a time-dependent study," *Phys. Rev. A* **94**, 063408 (2016).
37. J. Ortigoso, "Mechanism of molecular orientation by single-cycle pulses," *J. Chem. Phys.* **137**, 044303 (2012).
38. J. Wu and H. Zeng, "Field-free molecular orientation control by two ultra-short dual-color laser pulses," *Phys. Rev. A* **81**, 053401 (2010).
39. M. Yoshida and Y. Ohtsuki, "Orienting CO molecules with an optimal combination of THz and laser pulses: optimal control simulation with specified pulse amplitude and fluence," *Phys. Rev. A* **90**, 013415 (2014).
40. M. Spanner, S. Patchkovskii, E. Frumker, and P. Corkum, "Mechanisms of two-color laser-induced field-free molecular orientation," *Phys. Rev. Lett.* **109**, 113001 (2012).
41. C.-C. Shu and N. E. Henriksen, "Field-free molecular orientation induced by single-cycle THz pulses: The role of resonance and quantum interference," *Phys. Rev. A* **87**, 013408 (2013).
42. S.-L. Liao, T.-S. Ho, H. Rabitz, and S.-I. Chu, "Maximum attainable field-free molecular orientation of a thermal ensemble with near-single-cycle THz pulses," *Phys. Rev. A* **87**, 013429 (2013).
43. I. Znakovskaya, M. Spanner, S. De, H. Li, D. Ray, P. Corkum, I. V. Litvinyuk, C. L. Cocke, and M. F. Kling, "Transition between mechanisms of laser-induced field-free molecular orientation," *Phys. Rev. Lett.* **112**, 113005 (2014).
44. Y. Kurosaki, H. Akagi, and K. Yokoyama, "Dynamic discrimination of oriented molecules controlled with the nonresonant dynamic Stark effect induced by a single-cycle THz pulse," *Phys. Rev. A* **90**, 043407 (2014).
45. C. Qin, Y. Liu, X. Zhang, and T. Gerber, "Phase-dependent field-free molecular alignment and orientation," *Phys. Rev. A* **90**, 053429 (2014).
46. S. Trippel, T. Mullins, N. L. M. Müller, J. S. Kienitz, R. Gonzalez-Ferez, and J. Küpper, "Two-state wave packet for strong field-free molecular orientation," *Phys. Rev. Lett.* **114**, 103003 (2015).
47. S. Kallush and S. Fleischer, "Orientation dynamics of asymmetric rotors using random phase wave functions," *Phys. Rev. A* **91**, 063420 (2015).
48. D. Takei, J. H. Mun, S. Minemoto, and H. Sakai, "Laser-field-free three-dimensional molecular orientation," *Phys. Rev. A* **94**, 013401 (2016).
49. R. Damari, D. Rosenberg, and S. Fleischer, "Coherent radiative decay of molecular rotations: a comparative study of terahertz-oriented versus optically aligned molecular ensembles," *Phys. Rev. Lett.* **119**, 033002 (2017).
50. S. Fleischer, Y. Zhou, R. W. Field, and K. A. Nelson, "Molecular orientation and alignment by intense single-cycle THz pulses," *Phys. Rev. Lett.* **107**, 163603 (2011).
51. P. Babilotte, K. Hamraoui, F. Billard, E. Hertz, B. Lavorel, O. Faucher, and D. Sugny, "Observation of the field-free orientation of a symmetric-top molecule by terahertz laser pulses at high temperature," *Phys. Rev. A* **94**, 043403 (2016).
52. O. Ghafur, A. Rouzee, A. Gijbetsen, W. K. Siu, S. Stolte, and M. J. J. Vrakking, "Impulsive orientation and alignment of quantum-state-selected NO molecules," *Nat. Phys.* **5**, 289 (2009).
53. A. Goban, S. Minemoto, and H. Sakai, "Laser-field-free molecular orientation," *Phys. Rev. Lett.* **101**, 013001 (2008).
54. S. De, I. Znakovskaya, D. Ray, F. Anis, N. G. Johnson, I. A. Bocharova, M. Magrakvelidze, B. D. Esry, C. L. Cocke, I. V. Litvinyuk, and M. F. Kling, "Field-free orientation of CO molecules by femtosecond two-color laser fields," *Phys. Rev. Lett.* **103**, 153002 (2009).
55. E. Frumker, C. T. Hebeisen, N. Kajumba, J. B. Bertrand, H. J. Wörner, M. Spanner, D. M. Villeneuve, A. Naumov, and P. B. Corkum, "Oriented rotational wave-packet dynamics studies via high harmonic generation," *Phys. Rev. Lett.* **109**, 113901 (2012).
56. E. Frumker, N. Kajumba, J. B. Bertrand, H. J. Wörner, C. T. Hebeisen, P. Hockett, M. Spanner, S. Patchkovskii, G. G. Paulus, D. M. Villeneuve, A. Naumov, and P. B. Corkum, "Probing polar molecules with high harmonic spectroscopy," *Phys. Rev. Lett.* **109**, 233904 (2012).
57. D. Dimitrovski, M. Abu-samha, L. B. Madsen, F. Filsinger, G. Meijer, J. Köpper, L. Holmegaard, L. Kalhoj, J. H. Nielsen, and H. Stapelfeldt, "Ionization of oriented carbonyl sulfide molecules by intense circularly polarized laser pulses," *Phys. Rev. A* **83**, 023405 (2011).
58. R. Tehini, K. Hamraoui, and D. Sugny, "Shaping of the time evolution of field-free molecular orientation by THz laser pulses," *Phys. Rev. A* **99**, 033419 (2019).
59. D. Sugny, A. Keller, O. Atabek, D. Daems, C. M. Dion, S. Guérin, and H. R. Jauslin, "Laser control for the optimal evolution of pure quantum states," *Phys. Rev. A* **71**, 063402 (2004).
60. D. Sugny, A. Keller, O. Atabek, D. Daems, C. M. Dion, S. Guérin, and H. R. Jauslin, "Control of mixed-state quantum systems by a train of short pulses," *Phys. Rev. A* **72**, 032704 (2005).
61. M. Lapert, S. Guérin, and D. Sugny, "Field-free quantum cogwheel by shaping of rotational wave packets," *Phys. Rev. A* **83**, 013403 (2011).
62. M. Lapert, E. Hertz, S. Guérin, and D. Sugny, "Field-free permanent molecular planar alignment," *Phys. Rev. A* **80**, 051403 (2009).
63. U. Boscain, M. Sigalotti, and D. Sugny, "Introduction to the pontryagin maximum principle for quantum optimal control," *PRX Quantum* **2**, 030203 (2021).
64. E. Gershnel, I. S. Averbukh, and R. J. Gordon, "Enhanced molecular orientation induced by molecular antialignment," *Phys. Rev. A* **74**, 053414 (2006).
65. E. Gershnel, I. S. Averbukh, and R. J. Gordon, "Orientation of molecules via laser-induced antialignment," *Phys. Rev. A* **73**, 061401 (2006).